Asian Journal of Chemistry; Vol. 24, No. 9 (2012), 3837-3841

ASIAN JOURNAL OF CHEMISTRY

www.asianjournalofchemistry.co.in

A Novel Hydrogen Peroxide Sensor Based on Silver Nanoparticles Electrodeposited on PFS-DNA Networks Modified Glassy Carbon Electrode

Z.F. HE, Y.H. SONG, L. WANG*, L.L. WAN, H.Z. ZHU and S. GAO

College of Chemistry and Chemical Engineering, Jiangxi Normal University, 99 Ziyang Road, Nanchang 330022, P.R. China

*Corresponding author: Tel/Fax: +86 791 8120861; E-mail: lwangsy2003@hotmail.com

(*Received*: 23 May 2011; *Accepted*: 14 April 2012) AJC-11251

A novel hydrogen peroxide (H_2O_2) sensor based on the silver nanoparticles (Ag NPs) electrodeposited on a poly(ferrocenylsilane) (PFS)-DNA networks modified glassy carbon electrode (GCE) was successfully constructed. The electrochemical experiments showed that this Ag NPs/PFS-DNA/GCE had a good catalytic ability toward the reduction of H_2O_2. The effects of PFS-DNA layers, electrodeposition time for silver nanoparticles formation and the pH of the electrolyte solution on the electrocatalytic reduction of H_2O_2 were investigated. Under the optimal conditions, the sensor exhibited a linear range of 2.0 μM to 35.3 mM with the detection limit of 0.6 μM. A rapid response of the sensor could achieve 95 % of the steady-state current in less than 2 s. This sensor with a high selectivity and sensitivity was expected to use for practical applications in detecting H_2O_2.

Key Words: Sensor, DNA, Poly(ferrocenylsilane), Silver nanoparticles, Peroxide hydrogen.

INTRODUCTION

The accurate determination of hydrogen peroxide (H_2O_2) has attracted extensive interest because H_2O_2 is an essential mediator in food, pharmaceutical, clinic and environmental analysis. Electrochemistry technique has been extensively employed in the detection of H_2O_2 owing to its intrinsic sensitivity, high selectivity, low-cost and simplicity[1-5].

In electrochemical detection of H_2O_2, one focus is mainly played on the materials modified electrode, since the materials determine directly the sensitivity and selectivity of the sensors. Many proteins, showing a sensitive and selective electrocatalysis to the reduction of H_2O_2 due to its interior electroactive iron heme, have been used to modify electrode for the determination of H_2O_2[6-9]. However, it is a serious issue that the biological and electrochemical activity of these enzymes immobilized on electrode surface will lose easily. Compared to these heme proteins, some biological materials are attracting more and more attention owing to its stability and convenience of electron transfer, such as hexacyanoferrate[10], Prussian blue-modified gold nanoparticles[11], platinum nanoparticles[12-14], nickel hexacyanoferrate[15], perovskite-type oxide[16], inorganic-organic composite materials[17,18] and Ag NPs[19-22]. Among them, Ag NPs exhibits excellent catalytic-activity and high-selectivity toward the reduction of H_2O_2.

Another focus is mainly played on the construction of modified electrode, since the performance of the sensor depends strongly on the amount of effective catalyst and the electron transfer between the catalyst and electrode surface. To obtain a good catalytic ability from the view of the construction of modified electrode, some porous and conductive matrixes have been used to immobilize catalyst on electrode surface. For example, sol.gel networks containing gold nanoparticles[23] and vertically aligned gold nanowire[24] have been employed to immobilize horseradish peroxides for detection of H_2O_2. Electrodeposition of Ag^+ in a solution containing DNA molecules[19] and direct electrodeposition of Ag^+ on performed DNA networks[21] and performed collagen networks[22] to produce Ag NPs on electrode surface has been developed and the resulted sensor showed a good catalytic ability.

In this manuscript, Ag^+ was electrodeposited on three-dimensional (3D) poly(ferrocenylsilane) (PFS)-DNA networks to produce 3D Ag NPs networks and accordingly developed a novel H_2O_2 sensor. The DNA stacked base pairs could be considered as a system of connected π electrons to transfer electrons[25]. Poly(ferrocenylsilane) is an electroactive polyelectrolyte with positive charge and organometallic units in its backbone, belonging to the class of stimulus responsive materials[26]. When the first oxidation was accomplished, the PFS films could be partially swollen and thus counterions could diffuse into the films to facilitate the electron transfer in the next step. The degree of solvation of the films depends on the degree of oxidation and influenced the electrochemical behaviours. It was very important that PFS and DNA could form 3D porous configuration

and accordingly improve the electron and electrolyte ion transfer obviously[27,28]. Compared to some previous works, the resulted sensor showed a superior electrocatalytic behaviour to the reduction of H_2O_2. DNA played an important role as an intermediate for the absorption of PFS and electron transfer.

Atomic force microscopy (AFM) measurements were carried out with an AJ-III (Shanghai Aijian Nanotechnology) in tapping mode. Standard silicon (Si) cantilevers (spring constant, 0.6.6 N/m) were used under its resonance frequency (typically, 60.150 kHz).

EXPERIMENTAL

The λ-DNA was purchased from Shanghai Biotechnology Company (Shanghai, China). Poly(ferrocenylsilane) (PFS) was synthesized according to the reported method[29] and its structure was shown in inset of Fig. 1. Other chemical reagents were purchased from Beijing Chemical Reagent Factory (Beijing, China) and were of analytical reagent grade. All solutions were prepared with ultra-pure water purified by a Millipore-Q System (18.2 MΩ cm). A series of phosphate buffer solution (PBS, 0.2 M) was used as supporting electrolyte and was prepared by mixing solution of 0.2 M Na_2HPO_4 and 0.2 M NaH_2PO_4.

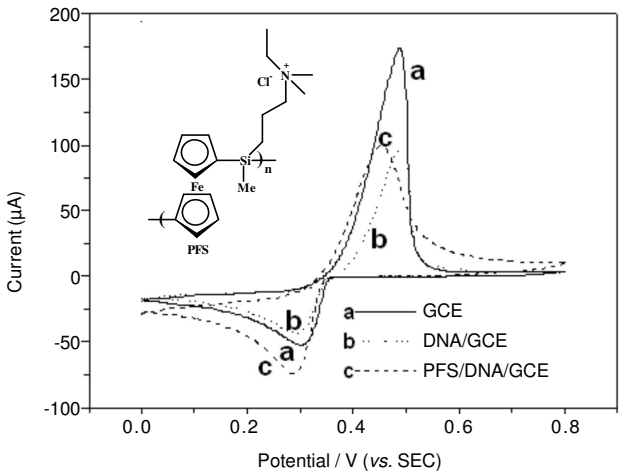

Fig. 1. CVs of the GCE (a), PFS/GCE (b) and (PFS-DNA)$_3$/GCE (c) in the solution of 3 mM $AgNO_3$ + 0.1 M KNO_3. Scan rate: 50 mV s^{-1}

Preparation of modified electrode: The polished glass carbon electrode (GCE) was immersed in DNA solution (100 ng/μL) at 4 ºC for 4 h. Then, the electrode was rinsed by ethanol and ultra-pure water to remove off weakly bound molecules, respectively. And then, the modified electrode was immersed in a 0.5 M NaCl solution containing 1.0 mM PFS at 4 ºC for 4 h and accordingly formed PFS-DNA/GCE. The assembly of DNA and PFS were alternated to formed (PFS-DNA)$_n$/GCE. Finally, the (PFS-DNA)$_n$/GCE was immersed in 0.1 M KNO_3 solutions containing 3.0 mM $AgNO_3$ and electrodeposited to obtain Ag NPs/(PFS-DNA)n/GCE.

All electrochemical experiments were performed by a CHI 660 C electrochemical workstation (CH Instruments, Shanghai, China) using a conventional three-electrode system with an Ag NPs/PFS-DNA/GCE as the working electrode, a platinum wire as the auxiliary electrode and a saturated calomel electrode (SCE) as the reference electrode. The cyclic voltammetric experiments were performed in a quiescent solution. The amperometric experiments were carried out in a continuous stirring solution using a magnetic stirrer.

RESULTS AND DISCUSSION

Electrodeposition of Ag NPs on (PFS-DNA)$_n$/GCE: Cyclic voltammograms (CVs) was utilized to monitor the electrodeposition of the Ag^+ at bare GCE, DNA/GCE and (PFS-DNA)$_3$/GCE. As shown in Fig. 1, the bare GCE showed a pair of typical redox peaks (curve a) corresponding to the reduction and oxidation of Ag NPs. After the DNA was assembled onto the electrode, the redox peaks were obviously smaller than that of the bare GCE due to the blocking effect of the DNA films (curve b). The blocking made the reduction of Ag^+ more difficult and accordingly slowed down the growth of Ag NPs. The (PFS-DNA)$_3$/GCE displayed a similar response but the peak potential shifted negatively and the peak to peak separation reduced remarkably (curve c) as compared to that of DNA/GCE. This may be ascribed to the 3D porous PFS-DNA networks which effectively promoted the transfer of Ag^+ and electron from the reduction of Ag^+. According to the above redox behaviours, the Ag NPs was electrodeposited in this solution for 100 s at -0.1 V to obtain Ag NPs modified electrode.

Atomic force microscopy (AFM) characterization of the sensor construction: The typical surface morphology of as-prepared Ag NPs/(PFS-DNA)$_3$/GCE was characterized by AFM and the results were shown in Fig. 2. As could be seen in Fig. 2a, (PFS-DNA)$_3$/GCE showed 3D network-like structure. The network structure could be further proven by its corresponding phase image (Fig. 2b). The porous structure could significantly increase the effective electrode surface and improve the diffusion of analytes into the film. After the Ag^+ was electrodeposited on the surface of (PFS-DNA)$_3$/GCE, some Ag NPs formed and uniformly dispersed on (PFS-DNA)$_3$/GCE as shown in Fig. 2c. The produced Ag NPs were *ca.* 4.6 nm (Fig. 2d) and were obviously smaller than that of on DNA/GCE[21].

Amperometric response to H_2O_2: In the presence of 1.0 mM H_2O_2 in 0.2 M PBS (pH 7.0), the Ag NPs/(PFS-DNA)$_3$/GCE showed an obvious current (curve d in Fig. 3) as compared with that of the bare GCE (curve a in Fig. 3), DNA/GCE (curve b in Fig. 3) and (PFS-DNA)$_3$/GCE (curve c in Fig. 3), suggesting that the current mainly resulted from reduction of H_2O_2 catalyzed by Ag NPs on electrode surface. The catalytic current was obviously enhanced at the Ag NPs/(PFS-DNA)$_3$/GCE (curve c in Fig. 4) as compared with that at Ag NPs/PFS/GCE (curve a in Fig. 4) and Ag NPs/DNA/GCE (curve b in Fig. 4), indicating the PFS-DNA networks might play a crucial role in the catalytic performance. As previously reported[20,21], the catalytic reduction of H_2O_2 mainly depended on the effective surface area of silver nanoparticles. Welch *et al.*[20] compared the amperometric responses of a macroelectrode with the same geometric surface area as an array of electrodes. The amperometric response of the electrode array with 1.0 μm, 100 and 10 nm was 20, 200 and 2000 times larger than that of the macroelectrode. Thus, the well catalytic activity of Ag NPs/(PFS-DNA)$_3$/GCE was ascribed to the 3D porous PFS-DNA networks which resulted in the formation and the homogenous

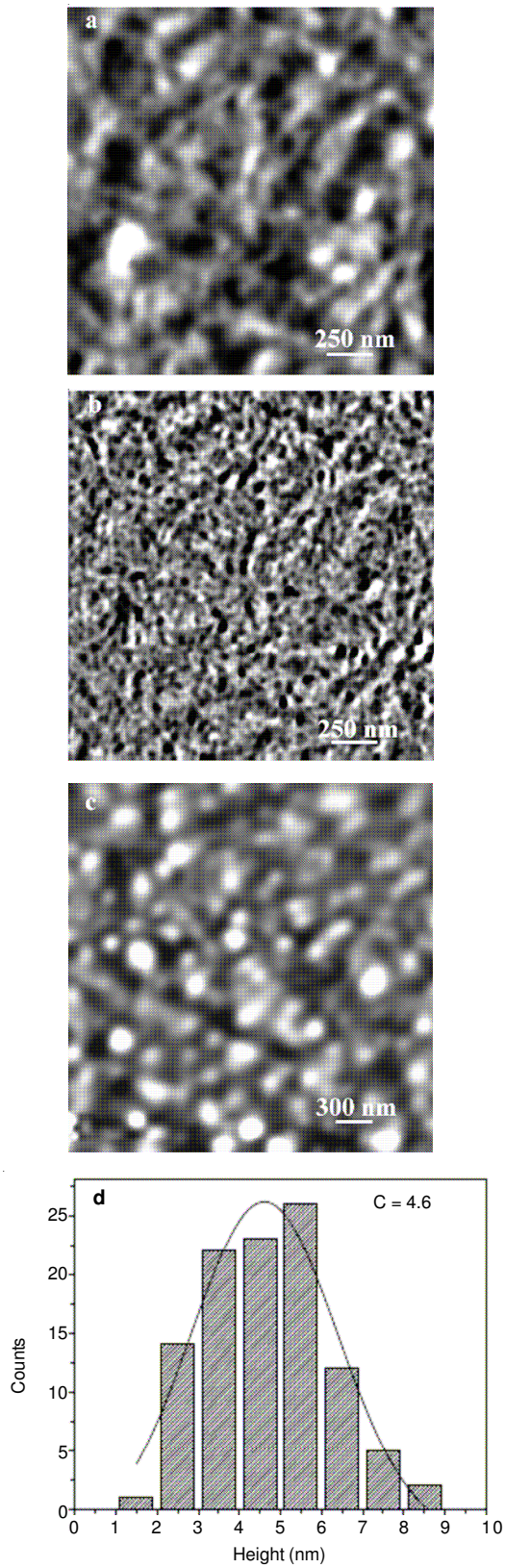

Fig. 2. AFM images of $(PFS\text{-}DNA)_3$/GCE (a height image; b phase image) and Ag NPs/$(PFS\text{-}DNA)_3$/GCE (c); (d) Histograms showing the size distribution of Ag NPs

distribution of a large number of small Ag NPs, which produced a larger effective surface area and accordingly produced more active sites on the same electrode surface in the NPs-assisted catalysis. The effective surface areas of different modified

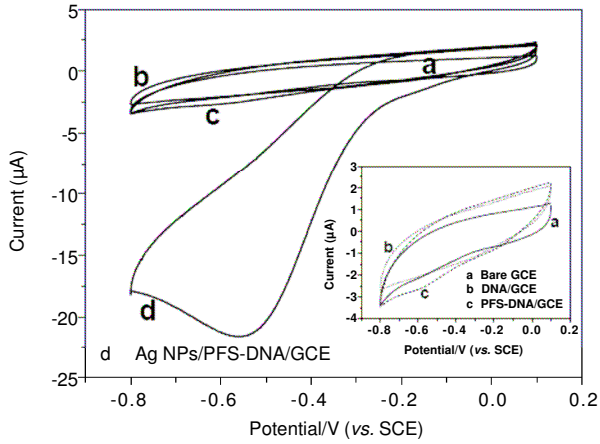

Fig. 3. CVs of bare GCE (a), DNA/GCE (b), $(PFS\text{-}DNA)_3$/GCE (c) and Ag NPs/$(PFS\text{-}DNA)_3$/GCE (d) in 0.2 M PBS (pH 7.0) in the presence of 1.0 mM H_2O_2. Scan rate: 50 mV s^{-1}. The inset was the enlarged curves of (a), (b) and (c)

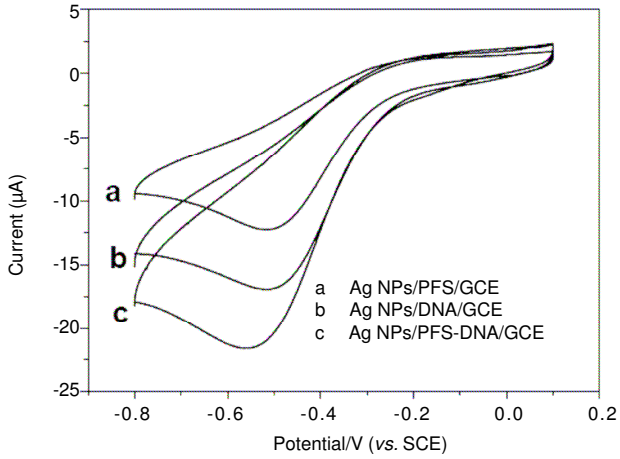

Fig. 4. CVs of the Ag NPs/PFS/GCE (a), Ag NPs/DNA/GCE (b) and Ag NPs/$(PFS\text{-}DNA)_3$/GCE (c) in 0.2 M PBS (pH 7.0) in the presence of 1.0 mM H_2O_2. Scan rate: 50 mV s^{-1}

electrode were estimated by the CVs obtained in 0.1 M KCl containing 5 mM $K_3[Fe(CN)_3]$ at a scan rate of 50 mV s^{-1}. The electroactive surface area (A_{eff}) of Ag NPs/GCE, Ag NPs/DNA/GCE, Ag NPs/PFS/GCE and Ag NPs/$(PFS\text{-}DNA)_3$/GCE were calculated to be 0.0784, 0.1312, 0.0583, 0.1953 cm^2, respectively (Table-1). Therefore, the Ag NPs/$(PFS\text{-}DNA)_3$/GCE showed a most remarkable catalytic response toward the reduction of H_2O_2. When these electrodes were used to detect H_2O_2, some key parameters such as detection limit and linear range were obtained (Table-1).

TABLE-1
COMPARISON OF THE KEY PARAMETERS OF THE DIFFERENT ELECTRODES

	A_{eff} (cm^2)	Linearity (mM)	Detection limit (μM)
Ag NPS/GCE	0.0784	0.05-9.3	16
Ag NPS/DNA/GCE	0.1312	0.005-15.9	1.8
Ag NPS/PFS/GCE	0.0583	0.01-11.35	3.0
Ag NPs/(PFS-DNA)3/GCE	0.1953	0.002-35.3	0.6

The possible electro-reduction mechanism was proposed as follows.

$$H_2O_2 + Ag \rightarrow 2H^+ + O_2 + 2e^- \quad (1)$$

$$H_2O_2 + 2e^- \rightarrow 2OH^- \quad (2)$$

$$2Ag(ox) + H_2O_2 \rightarrow 2Ag + 2H^+ + O_2 \quad (3)$$

$$Ag \rightarrow Ag(ox) + e^- \quad (4)$$

Optimization of experimental variables: To optimize the electrocatalytic performance of Ag NPs/$(PFS\text{-}DNA)_3$/GCE in 0.2 M PBS for reduction of H_2O_2, some factors related to the formation of sensor construction, such as layer number of PFS-DNA, electrodeposition time and pH, were investigated.

Since the layers of DNA-PFS played a critical role in the formation of Ag NPs and the catalytic ability to reduction of H_2O_2, the effect of layer of PFS-DNA on the catalytic current was first investigated and the result was shown in Fig. 5a. There was a remarkable increase in the current response with increasing the layers of DNA-PFS and the maximal value occurred at 3. After that, the steady-state current decreased gradually.

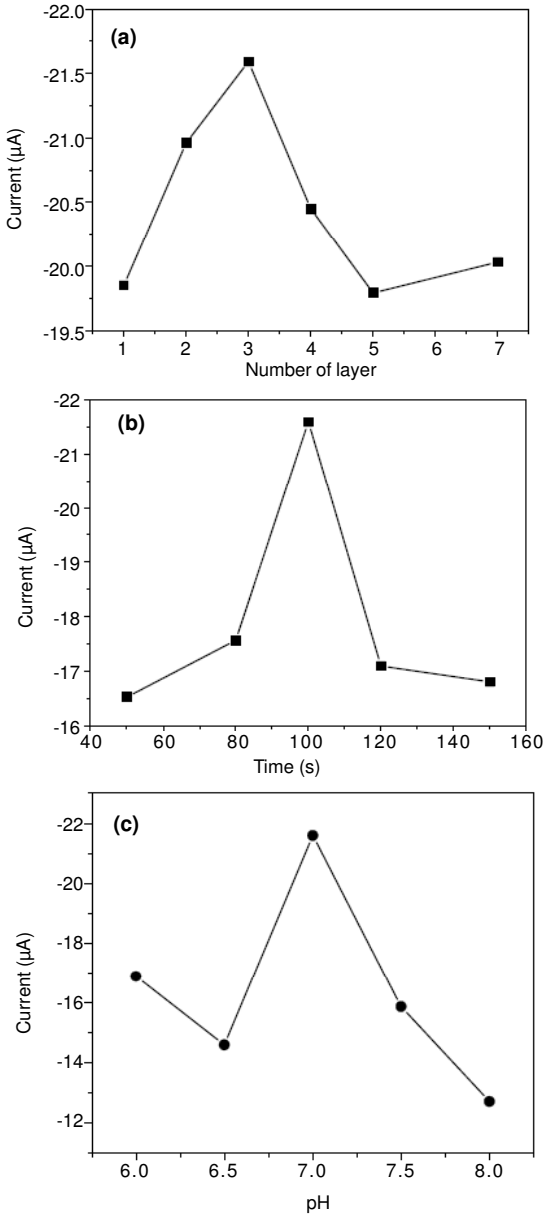

Fig. 5. Effects of number of layer (a), electrodeposition time (b) and pH (c) on the amperometric responses in 0.2 M PBS of pH 7.0 in the presence of 1.0 mM H_2O_2

Fig. 5b showed the effect of electrodeposition time on the electrocatalytic reduction of H_2O_2. The amperometric current response increased gradually with electrodeposition time increasing and reached the maximum value at 100 s. After that, the current response decreased gradually. This plot revealed that the 100 s was the optimal electrodeposition time for the preparation of the H_2O_2 sensor. This turning point might be due to the fact that Ag NPs would become rather bigger with the excessive electrodeposition time and accordingly reduced the effective surface area of Ag NPS, which might decrease its effective electrocatalytic sites on the Ag NPs.

The effect of the pH of electrolyte solution on the response of the sensor toward the reduction of H_2O_2 was also investigated. As shown in Fig. 5c, a better current response was obtained at pH of 7, which was similar with the physiological environment. The sensor was pH-dependent because the DNA could exist stably in the physiological environment and would damage easily in an acidic or alkaline condition. Thus, the PBS of pH 7 was chosen as the optimal electrolyte for the determination of H_2O_2.

Chronoamperometric response and calibration curve: The typical current.time curve of the sensor is shown in Fig. 6. The reduction current rose sharply to reach a maximum and achieved 95 % of the steady-state current within 2 s. The fast response was mainly attributed to the fact that the porous PFS-DNA networks facilitated the transfer of the H_2O_2 and the electron from the reduction of H_2O_2. The current increased linearly as the H_2O_2 concentrations increased from 2.0 μM to 35.3 mM (r = 0.9996; n = 18) (Fig. 6). The detection limit was estimated to be about 0.6 μM based on the criterion of a signal-to-noise ratio of 3. The comparison of the parameters of Ag modified electrodes as sensors for H_2O_2 detection with our results was also listed in Table-2.

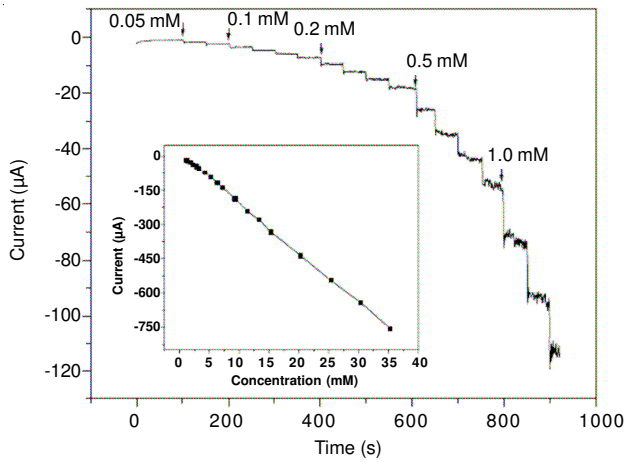

Fig. 6. Typical steady-state response of the sensor to successive injection of H_2O_2 into stirring 0.2 M PBS (pH 7.0). The inset was the calibration curve. Applied potential: -0.40 V

Selectivity and stability of the sensor: The selectivity of the sensor was evaluated as shown in Fig. 7. Two electroactive substances such as ascorbic acid (AA, 5.0 mM) and uric acid (UA, 5.0 mM) were injected into the PBS (pH 7.0) containing 1.4 mM H_2O_2, no obvious current was observed. This suggested that these species had no obvious interference in the detection of H_2O_2. The stability of the sensor was also

TABLE-2
COMPARISON OF THE PARAMETERS OF Ag MODIFIED ELECTRODES AS SENSORS FOR H_2O_2 DETECTION

	Response time (s)	Detection limit (μM)	Linear range (mM)	References
Ag-$Na_2Ti_3O_7$ NWs/GE	< 3	1.0	0.05-2.5	30
MWCNT/Ag nanohybrids/Au	–	0.5	0.05-17	31
Ag NPs/DNA/GCE	–	1.7	0.004-16	21
Ag NPs/type I collagen networks/GCE	–	0.7	0.005-40.6	22
Ag-DNA/GCE	–	0.6	0.002-2.5	19
Ag NPs/PFS-DNA/GCE	< 2	0.6	0.002 -35.3	This paper

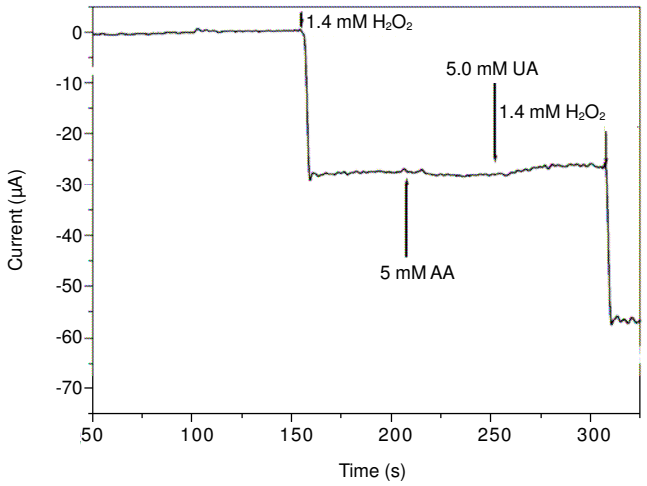

Fig. 7. Effects of ascorbic acid (AA) and uric acid (UA) on the amperometric responses of H_2O_2 in 0.2 M PBS of pH 7.0. Applied potential: -0.40 V

investigated in present work. After the sensor was stored in the inverted beaker at room temperature for 30 days, the current response to 1 mM H_2O_2 decreased only 1.2 % of the original current.

Conclusion

In summary, a novel H_2O_2 sensor based on Ag NPs electrodeposited on PFS-DNA network modified GCE was successfully constructed. When the electrodeposition time of Ag NPs was 100 s, the layer of PFS-DNA was 3 and the pH of PBS was 7.0, respectively, the resulted sensor showed the maximal electrocatalytic ability to the reduction of H_2O_2. The well catalytic activity of the Ag NPs/$(PFS\text{-}DNA)_3$/GCE was ascribed to the porous PFS-DNA network that resulted in the homogenous distribution of a large number of small Ag NPs. The resulted sensor showed a good electrocatalytic performance towards the reduction of H_2O_2 with an extremely fast amperometric response, a low detection limit, a wide linear range and a good selectivity.

ACKNOWLEDGEMENTS

This work was financially supported by National Natural Science Foundation of China (20905032, 21065005), Natural Science Foundation of Jiangxi Province (2008GZH0028), Foundation of Jiangxi Educational Committee (GJJ10389), the State Key Laboratory of Electroanalytical Chemistry (2008003) and the Scientific Research Foundation for the Returned Overseas Chinese Scholars, State Education Ministry.

REFERENCES

1. L. Bahshi, M. Frasconi, R. Tel-Vered, O. Yehezkeli and I. Willner, *Anal. Chem.*, **20**, 8253 (2008).
2. M. Riskin, R. Tel-Vered and I. Willner, *Adv. Funct. Mater.*, **19**, 2474 (2009).
3. T. Niazov, B. Shlyahovsky and I. Willner, *J. Am. Chem. Soc.*, **129**, 6374 (2007).
4. L. Wang and E. Wang, *Electrochem. Commun.*, **6**, 49 (2004).
5. Y. Song, L. Wang, C. Ren, G. Zhu and Z. Li, *Sensor. Actuat. B-Chem.*, **114**, 1001 (2006).
6. C. Guo, Y. Song, H. Wei, P. Li, L. Wang, L. Sun, Y. Sun and Z. Li, *Anal. Bioanal. Chem.*, **389**, 527 (2007).
7. D. Sarauli, J. Tanne, D. Schaer, I. W. Schubart and F. Lisdat, *Electrochem. Commun.*, **11**, 2288 (2009).
8. Y. Xu, C. Hu and S. Hu, *Sens. Actuators B*, **130**, 816 (2008).
9. C.Y. Liu and J.M. Hu, *Biosens. Bioelectron.*, **24**, 2149 (2009).
10. A. Eftekhari, *Talanta*, **55**, 395 (2001).
11. J.D. Qiu, H.Z. Peng, R.P. Liang, J. Li and X.H. Xia, *Langmuir*, **23**, 2133 (2007).
12. T. You, O. Niwa, M. Tomita and S. Hirono, *Anal. Chem.*, **75**, 2080 (2003).
13. R. Polsky, R. Gill, L. Kaganovsky and I. Willner, *Anal. Chem.*, **78**, 2268 (2006).
14. J. Li, W. Yang, H. Zhu, X. Wang, F. Yang, B. Zhang and X. Yang, *Talanta*, **79**, 935 (2009).
15. P. A. Fiorito and S.I. Cordoba de Torresi, *J. Electroanal. Chem.*, **581**, 31 (2005).
16. Y. Shimizu, H. Komatsu, S. Michishita, N. Miura and N. Yamazo, *Sens. Actuators B*, **34**, 493 (1996).
17. Z.M. Liu, Y. Yang, H. Wang, Y.L. Liu, G.L. Shen and R.Q. Yu, *Sens. Actuators B*, **106**, 394 (2005).
18. S. Hanaoka, J.M. Lin and M. Yamada, *Anal. Chim. Acta*, **426**, 57 (2001).
19. S. Wu, H. Zhao, H. Ju, C. Shi and Zhao, *J. Electrochem. Commun.*, **8**, 1197 (2006).
20. C.M. Welch, C.E. Banks, A.O. Simm and R.G. Compton, *Anal. Bioanal. Chem.*, **382**, 12 (2005).
21. K. Cui, Y. Song, Y. Yao, Z. Huang and L. Wang, *Electrochem. Commun.*, **10**, 663 (2008).
22. Y. Song, K. Cui, L. Wang and S. Chen, *Nanotechnology*, **20**, 105501 (2009).
23. J. Jia, B. Wang, A. Wu, G. Cheng, Z. Li and S. Dong, *Anal. Chem.*, **74**, 2217 (2002).
24. J. Xu, F. Shang, J.H.T. Luong, K.M. Razeeb and J.D. Glennon, *Biosens. Bioelectron.*, **25**, 1313 (2010).
25. E.M. Boon, N.M. Jackson, M.D. Wightman, S.O. Kelley, M.G. Hill and J.K. Barton, *J. Phys. Chem. B*, **107**, 11805 (2003).
26. M. Peter, R.G.H. Lammertink, M.A. Hempenius and G.J. Vancso, *Langmuir*, **21**, 5115 (2005).
27. Y.J. Ma, W.F. Dong, M.A. Hempenius, H. Mohwald and G.J. Vancso, *Angew. Chem. Int. Ed.*, **46**, 1702 (2007).
28. K. Cui, Y. Song and L. Wang, *Electrochem. Commun.*, **10**, 1712 (2008).
29. M.A. Hempenius, F.F. Brito and G.J. Vancso, *Macromolecules*, **36**, 6683 (2003).
30. X. He, C. Hu, H. Liu, G. Du, Y. Xi and Y. Jiang, *Sens. Actuators B*, **144**, 289 (2010).
31. W. Zhao, H. Wang, X. Qin, X. Wang, Z. Zhao, Z. Miao, L. Chen, M. Shan, Y. Fang and Q. Chen, *Talanta*, **80**, 1029 (2009).